Available online at www.sciencedirect.com

ScienceDirect

Procedia Structural Integrity 4 (2017) 87–94

Structural Integrity Procedia

www.elsevier.com/locate/procedia

ESIS TC24 Workshop "Integrity of Railway Structures", 24-25 October 2016, Leoben, Austria

# Determination of inspection intervals for welded rail joints on a regional network

S. Romano[a], S. Beretta*[a], G.S. Galli[b], R. Riccardo[b]

[a] POLItecnico di MIlano, Dept. Mechanical Engineering, Milan, Italy
[b] FERROVIENORD, Saronno, Italy

**Abstract**

One of the most frequent and dangerous failure modes in continuous welded rails is fatigue crack propagation terminated by brittle fracture. Due to the brittleness of the weld material and the scatter in its mechanical properties, a probabilistic approach is necessary. The paper deals with surface cracks at the foot base of aluminothermic welded rails, developing a probabilistic methodology for determining the day by day prospective failure probability. The model used is based on weld material characterization, simulation of fatigue crack growth and day-by-day failure probability calculation using the Monte Carlo method. The model is then adopted to assess the time dependent safety margin during fatigue crack propagation and to understand which variables are really influencing the failure probability. Finally, the results are compared to the standard rail classification method, considering the real traffic condition in several railway lines.



*Keywords:* Rails; Fatigue crack in welds; Failure probability; Residual lifetime; Thermite welds; Defects

## 1. Introduction

The introduction of continuously welded rails has considerably improved the problems of wear and dynamic overloads that were the main causes of failure with mechanically joined rails. However, the several benefits introduced by this technology are partially balanced by frequent brittle fatigue failures originating and propagating in the welds (see Welding Technology Institute of Australia (2006); Mutton and Alvarez (2003); Salehi et al. (2011)). One of the most common failure modes is the vertical failure caused by cracks originating from the heat affected zone at the weld foot. This failure mode is not critical for safety but rather for network availability.

The aim of the research project is to model said failure mode, in order to evaluate the effect of the variables involved and to improve the track maintenance. This was achieved in three main steps:

* Corresponding author. Tel.: +39-0223998246.
*E-mail address:* stefano.beretta@polimi.it


10.1016/j.prostr.2017.07.004

1. how to describe the structural integrity of a rail welded joints;
2. how to consider the probabilistic aspects in a simple yet affordable way;
3. to draw general conclusions by applying the approach to a regional network.

The complete definition of the model has already been published (see Romano et al. (2016)) and focuses on the first two steps. The goal of this paper is to summarize those results and to especially address the third topic.

**Nomenclature**

| | |
|---|---|
| $a$ | crack depth |
| $a_0$ | initial crack depth |
| $c$ | half crack length |
| CSA | airport service train |
| EFBH | equivalent flat bottom hole |
| FAD | failure assessment diagram |
| FE | finite element |
| $J_c$ | $J$-integral at the onset of cleavage fracture |
| K | overall SIF |
| $K_J$ | fracture toughness |
| $K_{Jc}$ | elastic-plastic equivalent SIF |
| $K_{max}$ | maximum daily SIF applied |
| $K_r$ | ordinate of the FAD diagram |
| $L_r$ | ligament yielding parameter |
| $P_f$ | failure probability |
| SIF | stress intensity factor |
| TAF | train high frequency |
| $T$ | temperature |
| $T_{min}$ | minimum daily temperature |
| $T_N$ | neutral temperature |
| WF | weight function |
| $\Delta K$ | cyclic K factor range (= $K_{max} - K_{min}$) |
| $\sigma_{app}$ | applied stress |
| $\sigma_Y$ | yield strength ($R_{p0,2}$) |

## 2. Life propagation model

### 2.1. Scheme of the problem

The finite element modelling of the problem is depicted in Fig. 2. The idea for the integrity assessment of the welded joint is to consider a prospective crack at the rail foot and located near the weld toe. The weld geometry was described as depicted in Fig. 2c and the stress state in this region was investigated by FE analysis (see Romano et al. (2016)).

The different loads acting on the rail weld are depicted in Fig. 1a and here summarized:

- bending stress given by the load spectra of the passing vehicles;
- thermal stress as a consequence of prevented extension or shrinking, depending on the difference between the neutral temperature $T_N$ and the environmental one (depicted in Fig. 2b);
- welding residual stress.

Considering fracture mechanics, a good approximation was achieved adopting a simplified geometry for a plate having the same height as the rail section. This was verified introducing a sub-model in the crack region (Fig. 2b). In this way, the SIF for a crack at the weld toe has been modelled with the same substitute geometry but considering the real state of stress at the weld toe (see Fig. 2d) and the WF solution by Wang and Lambert (1995). The comparison between WF and FE solutions showed a maximum error of 20% for cracks with $a > 2\ mm$ and $0.4 < a/c < 1$.

The overall applied SIF $K$ can finally be calculated superimposing the different loading conditions as in Eq. 1:

$$K = K_{axle\ load} + K_{thermal\ stress} + K_{residual\ stress} \tag{1}$$

a

b

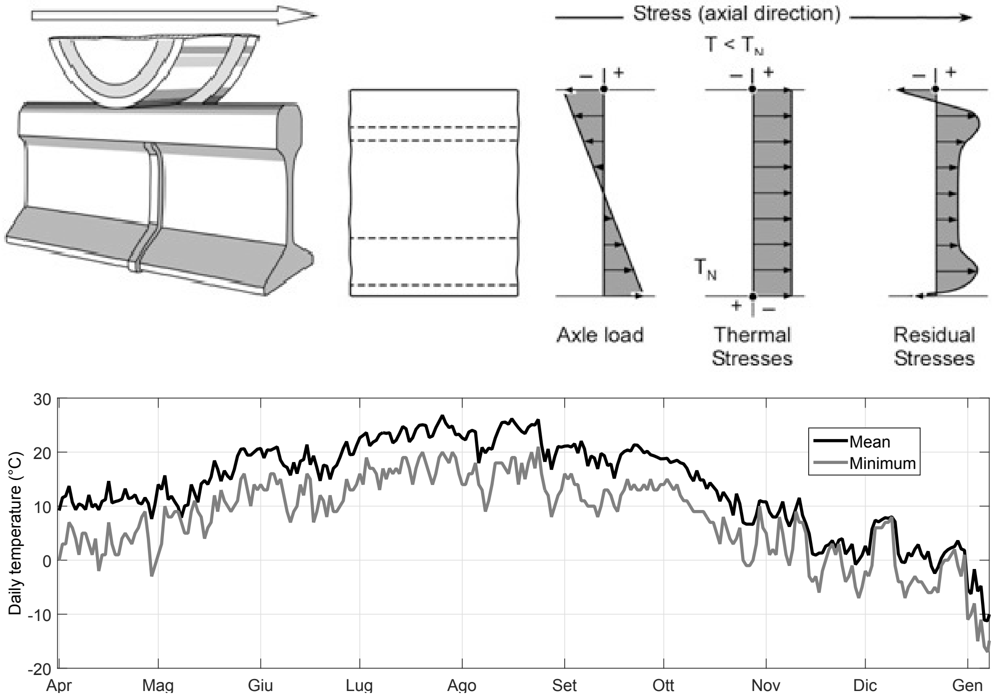


Fig. 1. (a) Different stress types acting on a welded joint ($T_N$ = neutral temperature); (b) daily mean and minimum temperature measured in the city of Saronno during the year, influencing the thermal stress.

### 2.2. Material characterization

The weld material has been characterized by a series of tests performed at different temperatures for determining: a) tensile properties; b) fracture toughness (Fig. 3a) crack growth rate at two stress ratios (Fig. 3b). In winter service conditions the welds are in the *lower shelf* and the material show a large scatter. Considering the fatigue crack propagation, the data were described using the NASGRO equation (see Romano et al. (2016) for the complete material description).

### 2.3. Integrity assessment

The integrity analysis has been done considering the real service conditions of a regional network (FERROVIENORD) in the Lombardia region. Traffic is mainly characterized by two types of trains: a rather heavy composed by 8 coaches for a full-weight capacity of 1800 kg (TAF, Fig. 4a) and a rather lightweight (CSA, Fig. 4b) composed by 4 coaches, 500 kg capacity. Firstly the analysis has considered quasi-static loads, depicted in Fig. 4c.

Assumptions for the analysis:

- initial crack size $a_0 = 0.9\ mm$ ($EFBH = 2\ mm$);
- crack propagation with $a/c = 0.4$ (which is the stabilized shape ratio).

The assessment against fracture is based on elastic-plastic driving force according to BS7910 (BS 7910 (2005)) format:

$$K_J = K/f(L_r) \leq K_{Jc} \tag{2}$$

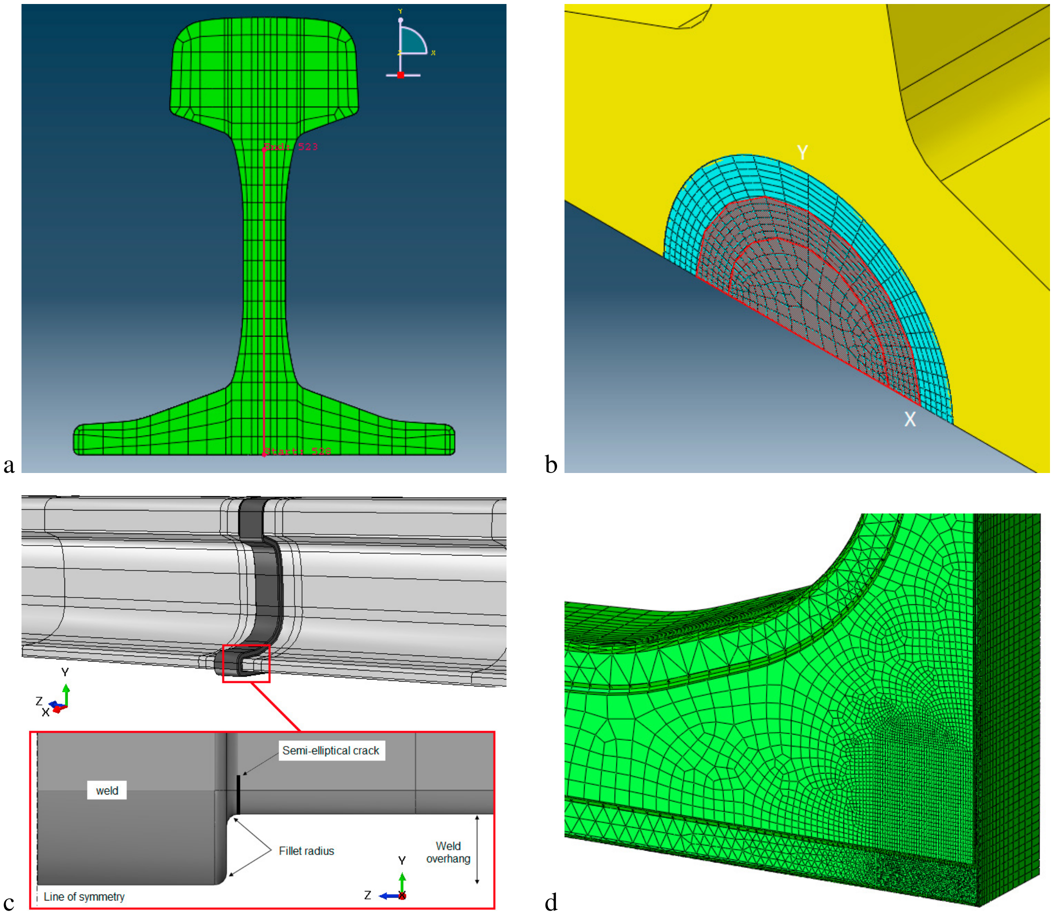


Fig. 2. Modelling of cracks at the rail foot (Romano et al. (2016)): (a) FE model of the rail; (b) sub-model of the crack for SIF calculation; (c) 3D model of weld geometry; (d) dense mesh in the crack region for stress calculation near the weld foot notch.

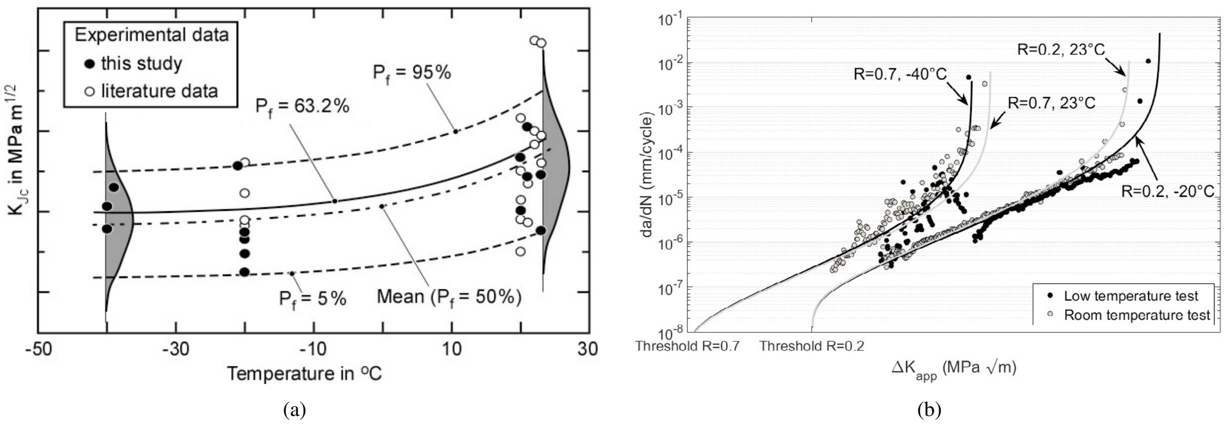


Fig. 3. Weld material properties Romano et al. (2016): (a) Master Curve for fracture toughness; (b) crack growth rate at different temperatures and stress ratios.

that leads to the FAD diagram. The material is expected to fail when

$$K_r = K/K_{Jc} > f(L_r) \tag{3}$$


Fig. 4. (a) TAF train; (b) CSA train; (c) quasi-static bending stress spectra.

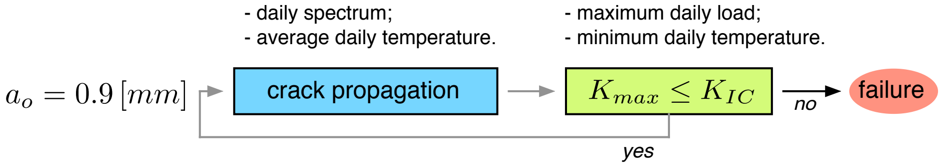


Fig. 5. Scheme of fatigue crack propagation and failure assessment.

where $L_r = \sigma_{app}/\sigma_Y$.

The scheme for the assessment is to follow the day-by-day crack propagation and to evaluate its potential failure as summarized in Fig. 5.

### *2.4. Semi-probabilistic approach*

The scatter related to the material description involves the necessity to adopt a probabilistic approach. Monte Carlo simulations were performed considering the distribution of the material properties measured experimentally. In particular, the yield strength is described by a Lognormal distribution with $CV = 0.02$, while the fracture toughness is well fitted by a three parameter Weibull and is the main variability of the problem (see Romano et al. (2016) for the details). Moreover, $K_{Jc}$ affects also the crack propagation rate at large applied SIFs, thus requiring a different crack propagation simulation for every single Monte Carlo extraction, as depicted in Fig. 6a. Finally, the load was introduced as a deterministic worst case described by the full-capacity spectra of the trains passing in the coldest moment of the day. At the end of every day crack propagation, the failure probability is calculated in the FAD for both the surface and depth crack tips (see the result for propagation day 1 and the first day in which $P_f > 1\%$ in Fig. 6b).

Given the long time required to run this complete model, a simple and fast simulation was adopted too. The hypothesis at the base is that day-by-day fatigue crack propagation is calculated considering a unique NASGRO curve, having a fixed fracture toughness. This value was set to a percentile of $K_{Jc}$ close to the failure probability under investigation, which in the particular case was 1%. The failure probability of each day is again calculated in the FAD as described above.

The Monte Carlo simulation for $10^6$ extractions has shown that the two approaches calculate the same result for a $P_f$ equal to the toughness percentile used for crack propagation (see the comparison in Fig. 6c).

## 3. Applications

### *3.1. Case histories*

If we consider a given daily spectrum (50 TAFs) it is easy to see the safety margin by simply plotting the day-by-day $K_{max}$ and to compare it with $K_{Jc}$ (Fig. 7).

Since almost all the weld failures happen in wintertime, it looks that the relevant parameter for the weld failures is the minimum temperature. In reality, failures happen also in warmer countries because the thermal load is given by

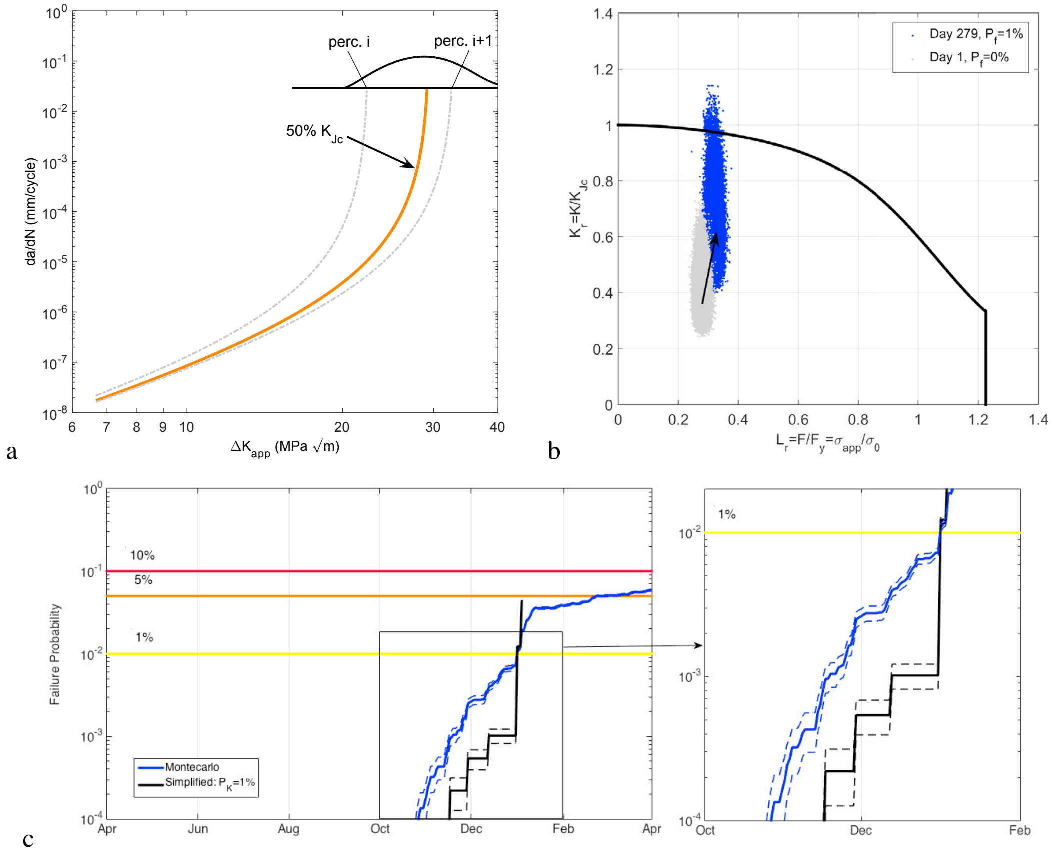


Fig. 6. (a) Random extraction for $K_{JC}$; (b) evolution on FAD; (c) Comparison between full Monte Carlo and simplified approach ($10^6$ extractions).

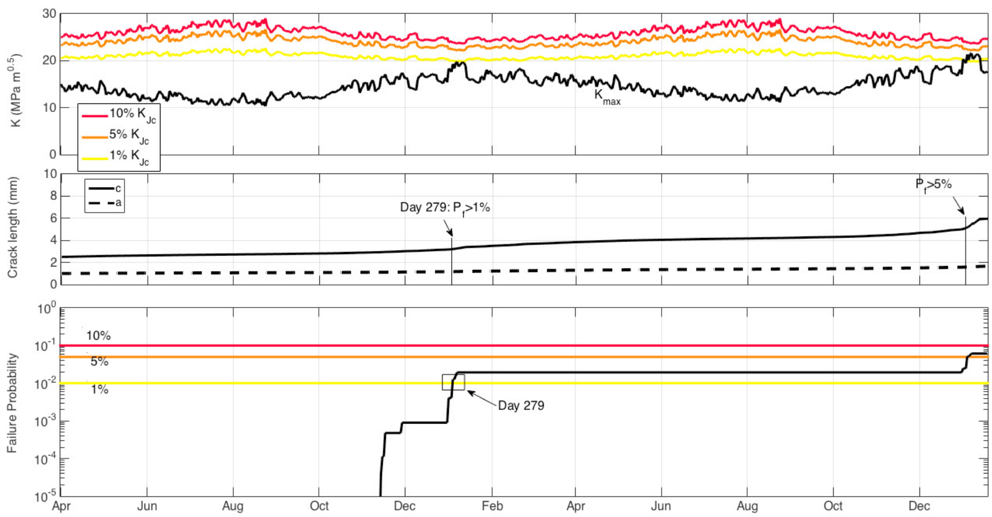


Fig. 7. Simulation of the propagation after a prospective inspection in April (50 TAFs per day, $a_0 = 0.9\,mm$, $a_0/c_0 = 0.4$)

the difference $(T_N - T_{min})$ (neutral temperature - minimum temperature). This was verified by considering different prospective locations with the same $T_N - T_{min}$.

Eventually, we have considered a propagation lifetime for the same daily tonnage, but caused by a few heavy TAF trains or by a large number of CSA (see Tab. 1). According to the standard UIC 714R (2009), the fatigue life to failure should be almost the same.

However, the propagation results are very different. The reason for this discrepancy is that $K_{max}$ plays a significant role, since we are in the lower shelf region, while UIC714R implicitly refers to $\Delta K$ as it was *plain* fatigue. This is not the case, since failure is controlled by $K_{max}/K_{Jc}$ and therefore the maximum stress during a time-history is the most critical event.

Table 1. Simulation of the propagation after a prospective inspection in April for two different train types ($a_0 = 0.9\,mm$, $a_0/c_0 = 0.4$).

| Train type | Train mass (t) | Trains per day | Line daily tonnage (t) | Life to failure (days) |
|---|---|---|---|---|
| TAF | 1.81 | 50 | 90.6 | 694 |
| CSA | 0.51 | 179 | 90.6 | 1016 |

### 3.2. Application to a regional network

The analysis tool has been adopted for predicting the propagation lifetime onto the regional network of FERROVIENORD Milano (FNM), shown in Fig. 8a. The network is characterized by trunks with a variety of tonnages, divided into three tonnage groups according to UIC 714R (2009).

The results reported in Fig. 8b show that, even if the lines have the same classification according to the standard, in some cases the propagation lifetime is very different.

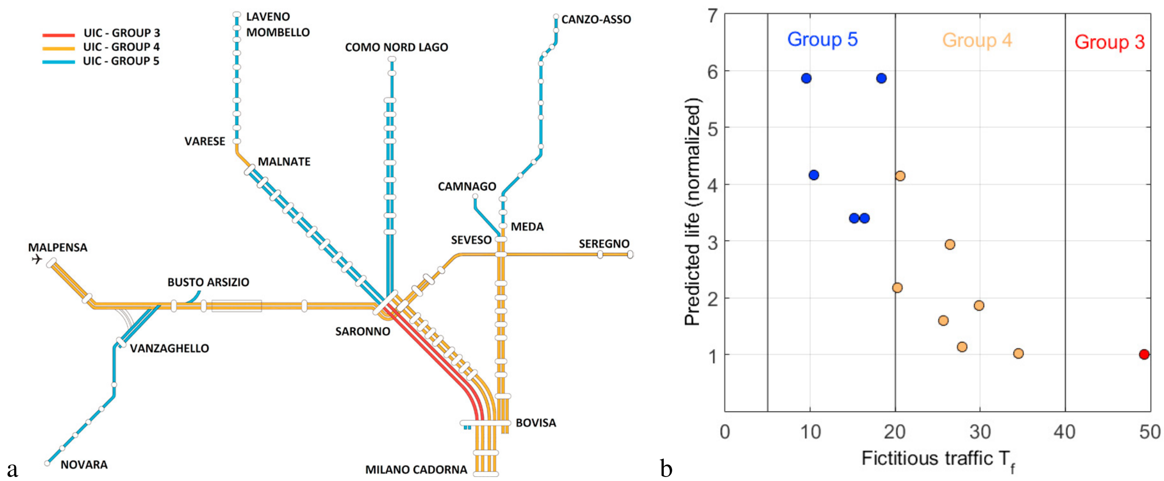


Fig. 8. (a) FERROVIENORD network examined; (b) propagation lifetime vs. daily tonnage.

This is confirmed by simulating for different stress spectra that refer to the same tonnage (see Fig. 9): in all cases, the expected life is lower when heavy trains pass on the line.

## 4. Conclusions

In this research we have set-up a probabilistic structural integrity model for the propagation lifetime of cracks at the weld toe of aluminothermic rail welds.

The conclusions that we can draw are:

- a propagation model should consider the different loads acting on the weld;
- below $0^oC$ the fracture toughness of welds is in the lower shelf and shows a significant scatter;

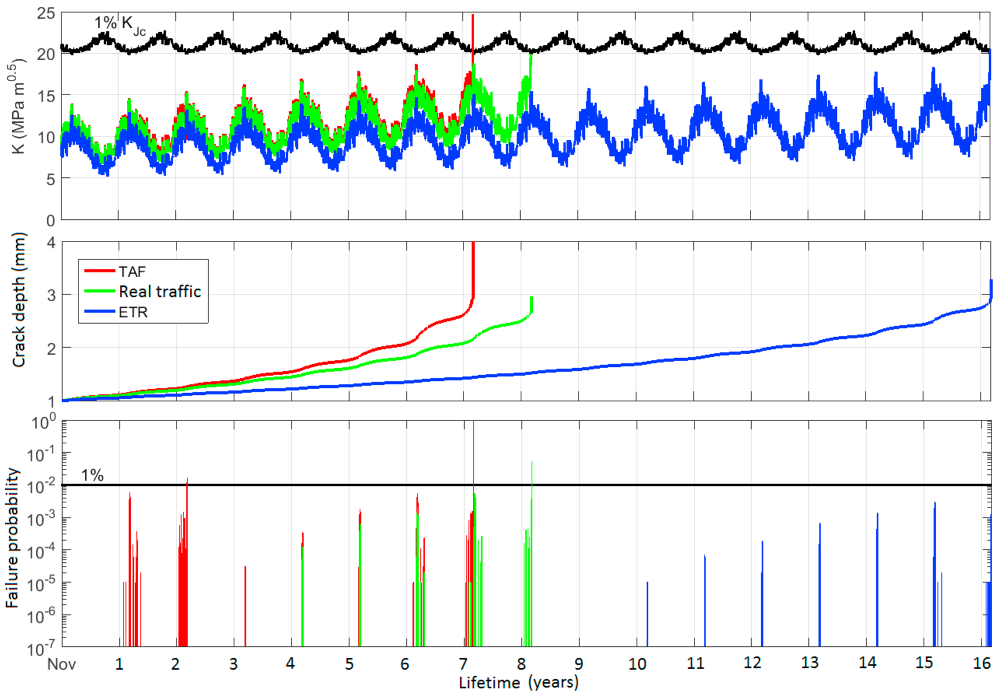


Fig. 9. Propagation lifetime for the same line (Saronno-Busto with real traffic and two different trains).

- the variability of the fracture toughness implies also a significant variability of the crack growth rate when $K_{max} \to K_{Jc}$;
- estimation of propagation lifetime needs a semi-probabilistic approach;
- results show that $K_{max}$ (and the maximum load) plays a significant role in determining the propagation lifetime;
- this fact prevents the application of a simple concept such as the tonnage of UIC714R standard.

## Acknowledgements

The research was carried out within a Research Contract between FERROVIENORD and Politecnico di Milano, Dept. Mechanical Engineering. The Authors acknowledge support from this contract and would like to thank Dr. Barra Caracciolo for the permission to publish the present results.

## References

BS 7910, 2005. Guide on methods for assessing the acceptability of flaws in metallic structures. British Standards.

Mutton, P., Alvarez, E., 2003. Failure modes in aluminothermic rail welds under high axle load conditions. Engineering Failure Analysis , 151–166.

Romano, S., Manenti, D., Beretta, S., Zerbst, U., 2016. Semi-probabilistic method for residual lifetime of aluminothermic welded rails with foot cracks. Theor. Appl. Fract. Mech. 85, 398–411. doi:10.1016/j.tafmec.2016.05.002.

Salehi, I., Kapoor, A., Mutton, P., 2011. Multi-axial fatigue analysis of aluminothermic rail welds under high axle load condition. International Journal of Fatigue 33.

UIC 714R, 2009. Classification des voies des lignes au point de vue de la maintenance de la voie. Technical Report.

Wang, X., Lambert, S., 1995. Local weight functions for semi-elliptical surface cracks in finite thickness plates. Theoretical and Applied Fracture Mechanics 23, 199–208.

Welding Technology Institute of Australia, 2006. Aluminothermic Weld Defects.